Original Research Paper   **Open Access**

3D Simulation Model of Tidal, Internal Mixing and Turbulent Kinetic Energy of Palu Bay

Sabhan*†, Alan Frendy Koropitan**, Mulia Purba*** and Widodo Setiyo Pranowo****

*Marine Science, Postgraduate Study Program, IPB University/Department of Physics, Faculty of Mathematical and Natural Sciences, Tadulako University, Indonesia, Perumahan Bumi Mallantan Rezkita Blok C2/1, Jl Roviega, Tondo, Palu City, Central Sulawesi, Indonesia
**Department of Marine Science and Technology, Faculty of Fisheries and Marine Science, IPB University, Jl.Raya Dramaga, Bogor 16680, West Java, Indonesia
***Department of Marine Science and Technology, Faculty of Fisheries and Marine Science, IPB University, Jl.Raya Dramaga, Bogor 16680, West Java, Indonesia
****Department of Hydrography, Indonesian Naval Postgraduate School (STTAL)/Researcher at Marine Research Center, Indonesian Ministry of Marine Affairs & Fisheries, Indonesia
† Corresponding author: Sabhan

ABSTRACT

The tidal simulation models and internal mixing were constructed using finite volume method to simulate diurnal tide (K1) constituent and semidiurnal tide (M2) constituent, the mixing level model using General Ocean Turbulence Model (GOTM). Tidal elevation amplitude of the model K1 ranges from 19.27 to 19.31 cm, high tidal amplitude at the point near the mouth of the Palu River, low tidal amplitude at the open boundary of the model that leads to the Makassar Strait. The amplitude range by M2 tidal constituents is 55.55-55.75 cm, high tidal amplitude at the mouth of Palu Bay and the end of Palu Bay and the slope area. The tidal current of the K1 constituent strengthens at the open boundary of the model and weakens into Palu Bay, which then undergoes strengthening near the mouth of the Palu River which experiences extreme siltation, tidal currents strengthen in the mouth area of Palu Bay and the tip of Palu Bay is caused by the tidal constituent propagation M2 and also the slope of the area along the coast of Palu Bay. Bottom Ekman layer which is caused by K1 constituent can reach 11 meters while the M2 constituent reaches 7 meters. In the slope area, are also found the buoyancy frequency with the order of 10-5 which is at a depth of 75-150 m. Kinetic energy in Palu Bay stands at O (10-5-10-3) with high kinetic energy around rough topography in the order of 10-3 around the mouth of Palu Bay.

INTRODUCTION

Palu Bay is administratively located in Donggala Regency, Palu City of Central Sulawesi Province. The position of Palu Bay is facing north with the bay mouth leading to the Makassar Strait, which is the main line of Indonesian Throughflow. The circulation of Palu Bay as semi-closed waters is strongly influenced by tides. Palu Bay has a unique morphology with a high depth degradation at a distance of 2000 meters from the coast, which can reach the depth of 300 meters or a slope of 25%. It is very potential for the occurrence of internal mixing on the slope. The process of seawater circulation is important to detect areas that have robust internal mixing in the management of the marine environment.

The depth of 450 meters in the mouth of Palu Bay allows the potential of Arlindo flow to affect the circulation in Palu Bay. At the end of the Palu Bay there is a major river that flows with an average discharge of 83.6 m^3/s with a

maximum discharge of 423 m^3/s which is possible to carry sediment of 0.42244 kg/s/m (Rusdin et al. 2014) from the upstream which are intensely experiencing land clearing for new agriculture land. This high level of discharge enables the potential nutrient transport into the Palu Bay.

Research on the 2D tidal circulation model in the bay area has been conducted by Carbajal & Backhaus (1998) with the semi-implicit method showing that tidal energy dissipation is found very strong in the delta. A 3D model study conducted by Koropitan & Ikeda (2008) with a larger scale on the Java Sea shows that the mixing is dominant by the K1 tidal constituent. Pichon & Correard (2006) modelled internal tides using a spring tidal constituent of daily tidal, showing that the vertical distribution of internal tidal amplitude is related to baroclinic propagations. Kartadikaria et al. (2011) conducted research in the Indonesian Sea using POM with (1/36)° resolution showing that vertical

mixing increased due to the effects of baroclinic pairs and increased horizontal mixing with the presence of barotropic tidal movements. Increased mixing has a role in eliminating high salinity water masses from the Pacific Ocean. Robertson & Field (2005) stated that in the Indonesian Sea significant M2 values of baroclinic tides were found on slope and rough topography, especially in the strait.

Tidal circulation modelling is an essential step to apply as it is being the main cause of internal mixing in the slope that occurs by reflection of M2 internal waves (Nash et al. 2004). Strong internal mixing indicates high primary productivity, although the internal mixing has insignificant contribution (10% to 25%) to primary productivity (Schafstall et al. 2010). Internal mixing causes nutrients to be mixed in the sediment so that they enter the upper water column which is then utilized by phytoplankton which is characterized by increased chlorophyll-*a* (McGowan & Hayward 1978, Pingree & Mardell 1981). Internal mixing is a mechanism for lifting nutrients to the surface in increasing primary productivity (Sharples et al. 2001, Holt et al. 2012). In the previous study, the focus was on regional areas, while this study focused on more detailed areas with a grid size of 100 m so that small degradation could be clearly identified.

This research simulates hydrodynamics in 3D, which is driven by wind and tides by using numerical models of finite volume. The result is verified by using measurements of currents and tides. This study investigates significant tidal constituents and its role to the mixing level. The total turbulent kinetic energy and dissipation in the domain model area are also computed.

MATERIALS AND METHODS

Description of the study sites: This research was conducted in Palu Bay, Central Sulawesi Province, Indonesia. Palu Bay is located on the Arlindo line in the Makassar Strait and the input of the Palu River is large during the rainy season. Rainfall patterns in the Palu bay fall into the category of Local Rain Patterns with only one (unimodal) peak season with an average annual rainfall of 547 mm, the lowest in all of Indonesia with the peak of the rainy season in June (Bayong 1999). Palu Bay provides environmental quality with human activities as the central government of Central Sulawesi Province (Fig. 1).

Hydrodynamic model, turbulent and validation: Hydrodynamic modelling in Palu Bay using 3D MOHID uses a finite volume approach to discretize equations (Neves 2007). MOHID 3D is a hydrodynamic model based on the Navier-Stokes equation with a Boussinesq and hydrostat-
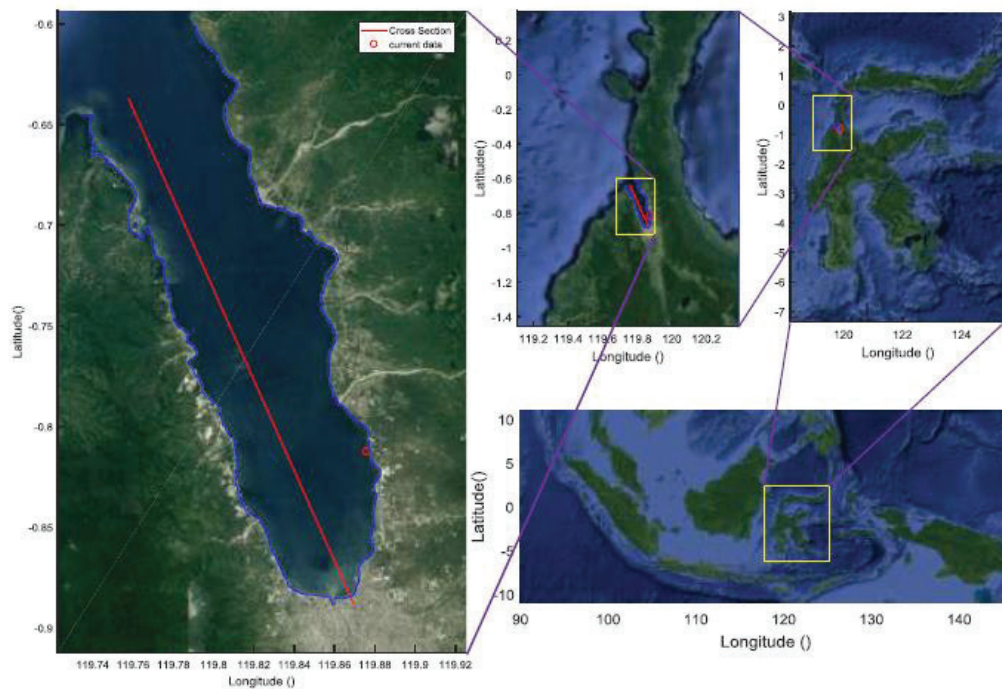

Fig. 1: the location of Teluk Palu, Central Sulawesi Province, Indonesia.

ic approach. 3D MOHID is formulated in a volume up to vertical discretization approach using sigma coordinates (Neves 2007). The open boundary of the model which is the generator input point for the tidal mouth model of Palu Bay leading to the Makassar Strait uses tidal constituents from FES2004. The study was carried out in Palu Bay (Fig. 1) by building a model that covers the entire water body of the Palu Bay. Turbulence modelling was carried out using a module (GOTM) which has been integrated with MOHID (Baumert et al. 2005) using the κ-∈ model approach (Versteeg & Malalasekera 2007).

Horizontal turbulence is calculated using a Smagorinsky turbulence model based on grid size and local derivative:

$$\nu_H = \Delta x \Delta y \sqrt{\left(\frac{\partial u}{\partial x}\right)^2 + \left(\frac{\partial v}{\partial y}\right)^2 + \frac{1}{2}\left(\frac{\partial u}{\partial x} + \frac{\partial v}{\partial y}\right)} \qquad \dots(1)$$

Equation (1) in MOHID has an expression in the form (Marín et al. 2013):

$$\nu_H = Horcon \times \Delta x \times \Delta y \sqrt{\left(\frac{\partial u}{\partial x}\right)^2 + \left(\frac{\partial v}{\partial y}\right)^2 + \frac{1}{2}\left(\frac{\partial u}{\partial x} + \frac{\partial v}{\partial y}\right)} \quad \dots(2)$$

Where, Horcon = 2.5 (Marín et al. 2013), is a dimensionless calibration constant.

Turbulence parameters in the form of vertical eddy diffusion by internal waves are calculated by the following equation (Gargett & Holloway 1984):

$$K_z = \frac{R_f}{1 - R_f} \frac{\varepsilon}{N^2} \qquad \dots(3)$$

Where, R_f is the Richardson number flux (0.20). Vertical displacement is obtained from the equation (Wang et al. 2018):

$$APE = \frac{g\rho'}{2\rho_c N^2} \qquad \dots(4)$$

Where, g is gravity acceleration, ρ is the perturbation density, ρ_c is the reference density, and N is the buoyancy frequency.

The grid cell size is $0.001° \times 0.001°$. As many as 14 main constituents of tidal (Mf, Mm, Msqm, Mtm, O1, P1, Q1, K1, M2, K2, 2N2, N2, S2 and M4) are used as tidal generators at the open boundary, and these constituents are derived from the tide model FES2004 global tide (Lyard et al. 2006). Tidal data were also obtained from the Pantoloan Port station operated by the Geospatial Information Agency (BIG). Bathymetry data were obtained from the Navy Base (Lanal) Palu with a grid of 20×20 meters (not accommodating bathymetry changes by the 2018 earthquake and tsunami incident).

Model Analysis: Characteristics of water level by tides and tidal currents resulting from the model based on the tidal harmonic constants of the two dominant tidal constituents (M2 and K1) were analysed with T_TIDE program (Pawlowicz et al. 2002).

RESULTS

Validation of model: The model was run for 30 days and validated with the results of tidal measurements from the Geospatial Information Agency (BIG) in Pantoloan Port for January (Table 1), the velocity of the model results was validated with the results of measurements at Donggala Beach (Fig. 2). K1 tidal constituent has the greatest contribution to the occurrence of discrepancies between the results of observation (Fig. 2) and results of model with the difference in amplitude and phase respectively 2.41 cm and -12.17 (Table 1).

Tidal Simulation

Tidal constituent K1: The amplitude, phase, and tidal currents of the K1 constituent are calculated for each 5 grids. Co-amplitude, co-phase and elliptical tidal currents of the K1 constituent are shown in Fig. 3a. The co-amplitude pattern and co-phase show a high tidal amplitude pattern at the end of the bay compared to the mouth of Palu Bay, while the phase propagates from the bay mouth who experience resonance in the middle of the bay due to the reflection of the wave returning from the end of the bay. The tidal eleva-

Table 1: Comparison of amplitude and phase between data from BIG and model results.

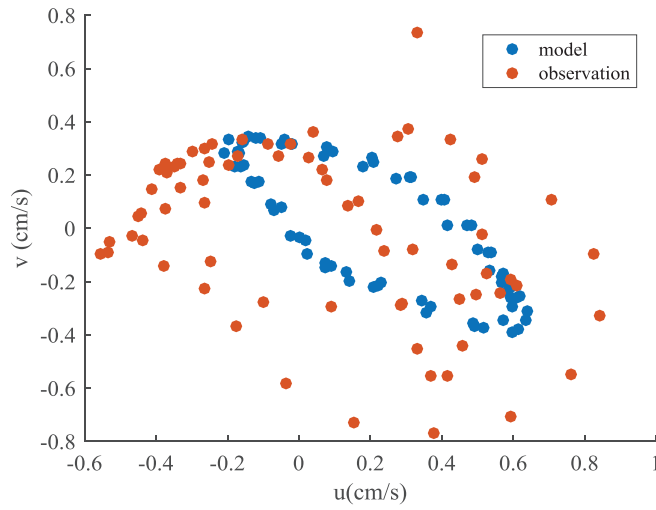| Constituent	Amplitudes (cm)			Phase (°)		
	Model	BIG Data	ΔH	Model	BIG Data	ΔHO1
ΔHO1	15.48	16.35	-0.87	128.09	131.57	-3.48
K1	19.06	21.47	-2.41	138	150.17	-12.17
M2	54.38	55.1	-0.72	284.09	282.38	1.71
S2	42.97	42.05	0.92	337.83	332.74	5.09

Fig. 2: Zonal and meridional current velocity plots between tidal currents of observation results (red) and model results (blue).
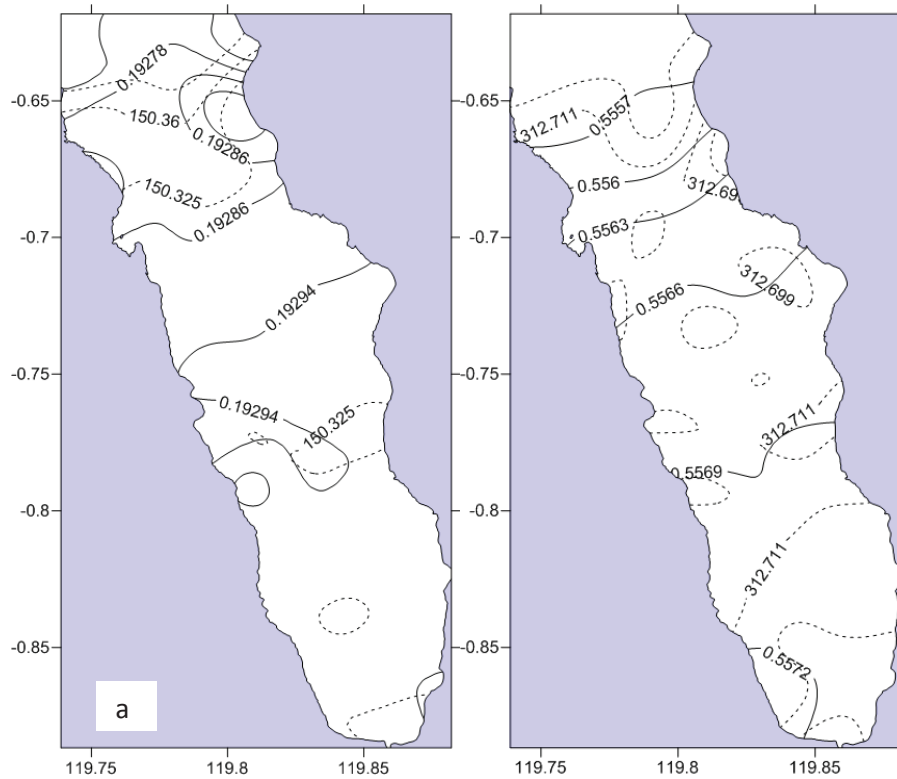

Fig. 3: Co-amplitude (cm) and Co-phase (°) (a) tidal constituent of K1, (b) tidal constituent of M2, amplitude (solid line) co-phase (dashed line).

tion amplitude of the K1 model results ranged from 19.27 to 19.31 cm high amplitude at points close to the mouth of the Palu River and low at the open boundary of the model leading to the Makassar Strait.

Co-phase model results show that the tidal wave propagates from the open boundary of the model in the Makassar Strait entering the bay until it reaches the end of the bay at the Palu river mouth with tidal co-phase from 150.3-150.42°.

Tidal current constituent K1 is presented from the model results for the surface (Fig. 4b) and bottom (Fig. 4a) of the waters in Palu Bay. The pattern of velocity of tidal currents of the K1 constituent strengthens at the open boundary of the model and weakens into the Palu Bay, which then undergoes strengthening at a certain point near the estuary which experiences extreme silting, the pattern between the speed on the surface and the bottom of the waters resembles only the 25% stronger surface compared to velocity at the bottom.

The average current velocity of the K1 constituent model results shows that there was a fairly strong current heading north near the east coast of the bay with a velocity of about 0.5 m/s in January 2016, the same as the research conducted by Sabhan et al. (2019). A strong K1 constituent

velocity is also found in the area near the mouth of the Palu Bay in a shallow topographic area (Fig. 6a).

Tidal constituent M2: Elliptical parameters of tidal currents by tidal constituents M2 was calculated for every 10 grids. Co-tidal is shown in Fig. 3b, referring that the M2 constituent fluctuates from the open boundary of the model at the mouth of Palu Bay then strengthens at the mouth of the Palu River at the end of the bay so that the co-amplitude is low in the centre of the bay, the amplitude range of M2 tidal constituents are 55.55 - 55.75 cm. Fig. 3b shows that the high amplitude in the bay mouth area, at the bay end and the slope areas which are close to the beach.

The velocity of the tidal current represented by the tidal current ellipse by the M2 constituent shows the same pattern between the surface and the bottom of the waters, but at the latter is weakened due to friction with the bottom of the waters (Fig. 5a). Tidal currents strengthened in the bay mouth area and the gulf tip (Fig. 5b) by the M2 tidal constituent propagation and the slope areas along the coast of Palu Bay. That corresponds to the results of research on the Hawaiian Sea backs that experienced siltation (Merrifield & Holloway 2002). Because Palu Bay only opens towards the Makassar Strait, the tidal propagation of M2 constituents comes from the Makassar Strait.
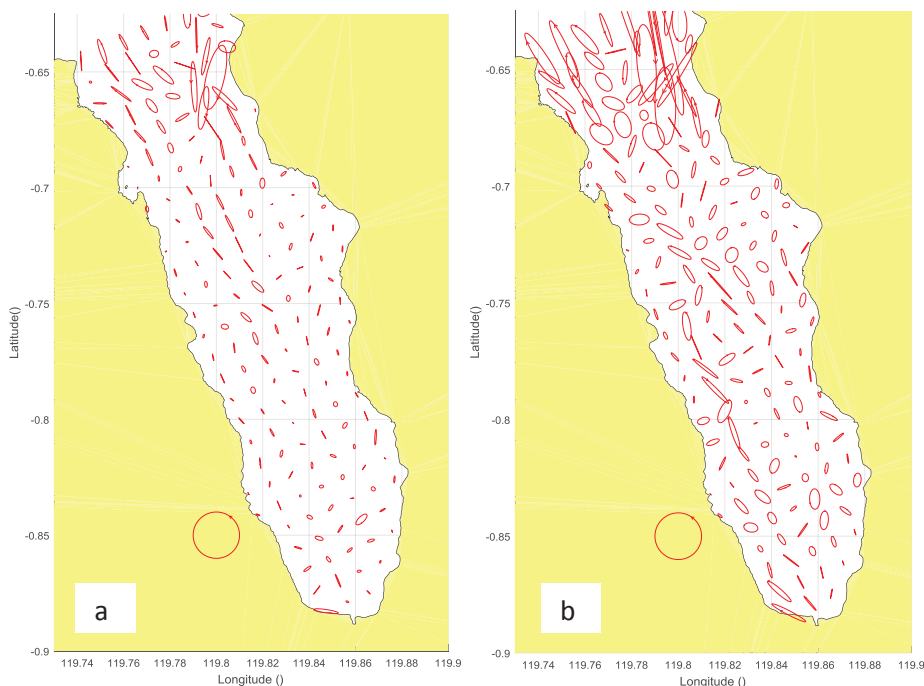

Fig. 4: Tidal current ellipses for K1 constituent (a) bottom (b) Surface.
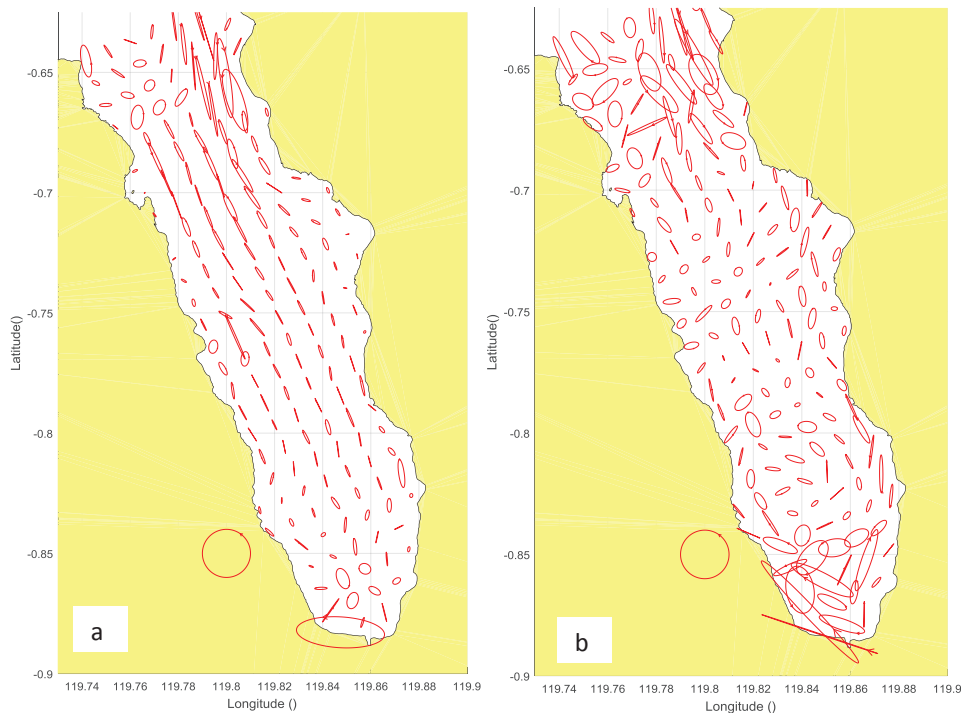
Fig. 5: Tidal current ellipses for M2 constituent (a) bottom, (b) Surface.

A strong M2 constituent velocity was also found in the area near the estuary of Palu Bay in a shallow topographical area (Fig. 6b). The M2 constituent pattern is almost the same as the K1 constituent pattern but the M2 constituent is stronger than the K1 constituent. Besides that, it is found that a fairly strong average current velocity reaching 1 m/s near the Palu River estuary is occurring in an area with low depth. Robertson & Field (2005) found that in the Indonesian Sea strong M2 baroclinic tides were present on the slope and rough topography especially in the strait.

Turbulent Models

Buoyancy frequency: The results of the model show that the buoyancy frequency (Brunt-Väisälä frequency) is in order $(10^{-1}-10^{-9})$ s^{-2}. The cross section intersecting the y axis that passes through the end of Palu Bay (estuary of Palu River) to the mouth of Palu Bay (Makassar Strait) shows that the frequency of buoyancy is high in the bay area, which is close to the river mouth, where the input of high river water forms a strong stratification by difference density. This result corresponds to the results of the study by Hordoir et al. (2018) which states that high buoyancy frequency values are present under strong stratification conditions. In the slope area also found areas with the order 10^{-5} which are at a depth of 75-150 m with a depth of

about 25 m from the bottom of the waters (Fig. 11a), this occurs because the slope area is a region with high friction (Wunsch 1968).

Turbulent dissipation: Fig. 10a shows the turbulent dissipation distribution pattern near the bottom in the Palu Bay. Fig. 11b shows that turbulent dissipation in the slope area is at O $(10^{-5}-10^{-4})$, whereas in areas with rough topography there is a turbulent dissipation area that is small, but higher one to two orders from the surrounding environment. These results are consistent with the results of the model conducted by Nikurashin et al. (2013) which states that in the absence of rough topography, internal turbulent mixing will decrease. As for the ocean with small tidal currents, internal wave friction is the dominant cause of turbulent dissipation (Ledwell et al. 2000, Jayne & St Laurent 2001).

Eddy diffusivity: Vertical slice of vertical eddy diffusivity on the y = 33 axis (Fig. 11c) has a fairly wide order with $(10^{0}-10^{-9})$, areas that have high eddy diffusivity in areas close to coarse topography with O $(10^{-3}-10^{-2})$ and the surface area, in the mouth area of the Bay found a high diffusivity area with first order where the incoming tidal currents hit the rough topography. According to the results of the study (Toole et al. 1994), increased dissipation was
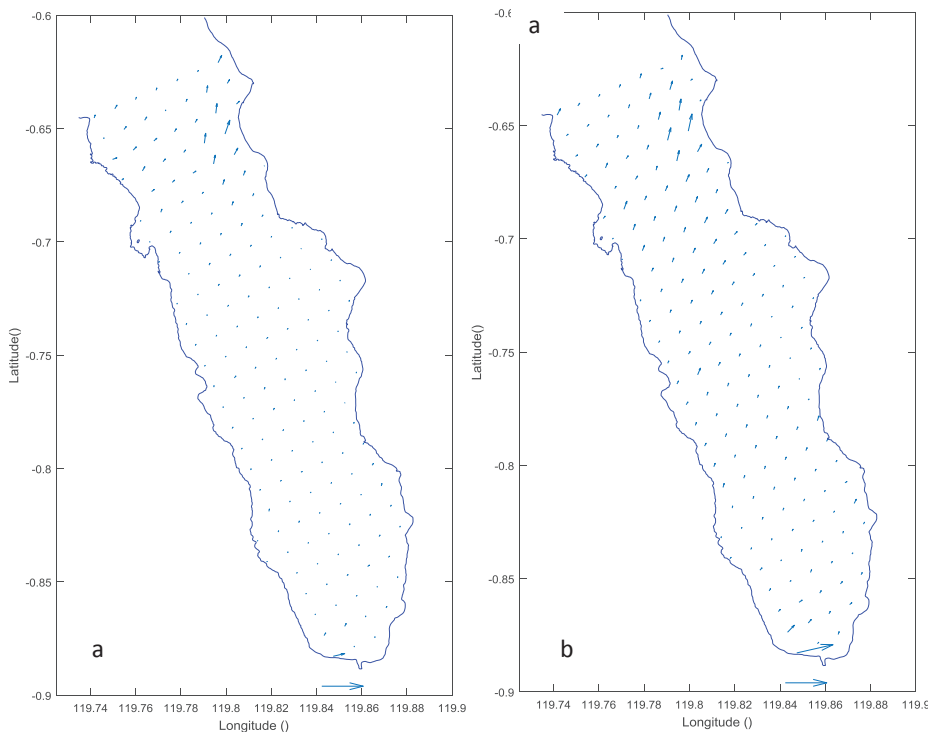
Fig. 6: The average velocity vector of (a) K1 constituent, (b) M2 constituent.

observed in the areas near steep boundaries (eddy diffusivity $>10^{-4}$ square meters per second).

Bottom friction velocity: Bottom friction velocity was calculated using equations (Zhurbas et al. 2018):

$$u^* = \left(\tau/\rho\right)^{0.5} \qquad \ldots(5)$$

$$\tau = \rho C_d u^2 \qquad \ldots(6)$$

Where, τ is the basic shear stress, ρ is the density of seawater. Fig. 8, the bottom friction velocity distribution for the tidal K1 and M2 constituents shows that the basic friction velocity of K1 constituent (Fig. 8a) has increased at a point where there is a rough topography, but is rapidly weakened, while the M2 constituent (Fig. 8b) speeds up from the bay mouth until reach the middle of the bay. High velocity is also found at the end of the bay due to silting or slope plus the flow of the river at the mouth of the Palu River. Sea threshold topography causes constriction, increasing the velocity of basic friction, this implies an increase in mixing on the other side of the sea threshold topography (Xing & Davies 2009).

Delta Ekman layer: Delta Ekman layer is calculated using equation (He & Weisberg 2002):

$$\delta = \frac{cu^*}{\sigma + f} \qquad \ldots(7)$$

Where, c = 0.2-0.4, σ is the tidal frequency and f is the tidal parameter. The M2 tidal frequency for Palu Bay is 2 times the frequency of the coriolis parameter so that the Ekman layer for the tidal constituent of M2 becomes: $\delta = \frac{cu^*}{3f}$.

Fig. 9 shows that the Ekman layer by the K1 constituent (Fig. 9a) can reach 11 meters, while the M2 constituent (Fig. 9b) reaches 7 meters. The point undergoes a high layer Ekman on the rough topography of the north side of the mouth of Palu Bay. But what is effective in mixing is in the slope section where the sea is getting shallow and the layer Ekman is getting bigger so that the mixed layer from the base is getting higher, in the next study this area has the potential to supply nutrients to the water column.

Energy flux is calculated using the equation:

$$\left(E_x, E_y\right) = \frac{\rho_0}{T} \int\limits_0^T \int\limits_{-h}^{\eta} (u,v)\left[g\eta + \frac{u^2 + v^2}{2}\right]dzdt \qquad \ldots(8)$$

Where, E_x and E_y are each flux energy of the constituent vector x and y, (u, v) is the vector of horizontal velocity,
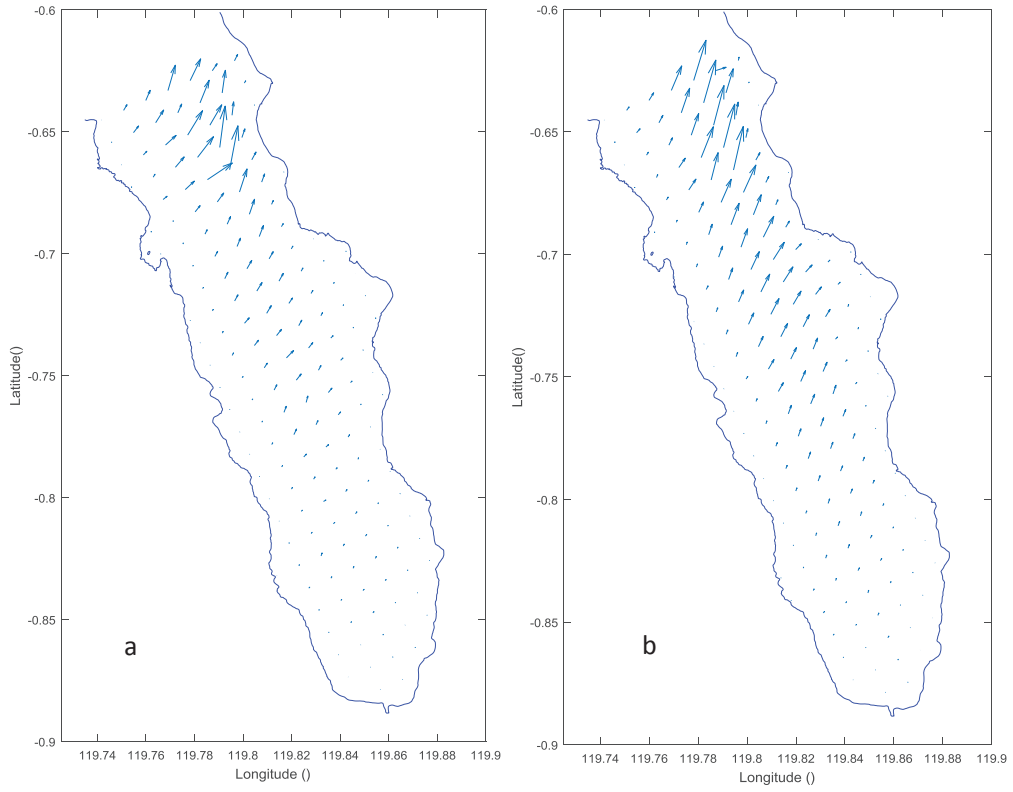
Fig. 7: Energy flux of Palu Bay by (a) tidal constituent K1, (b) tidal constituent M2.
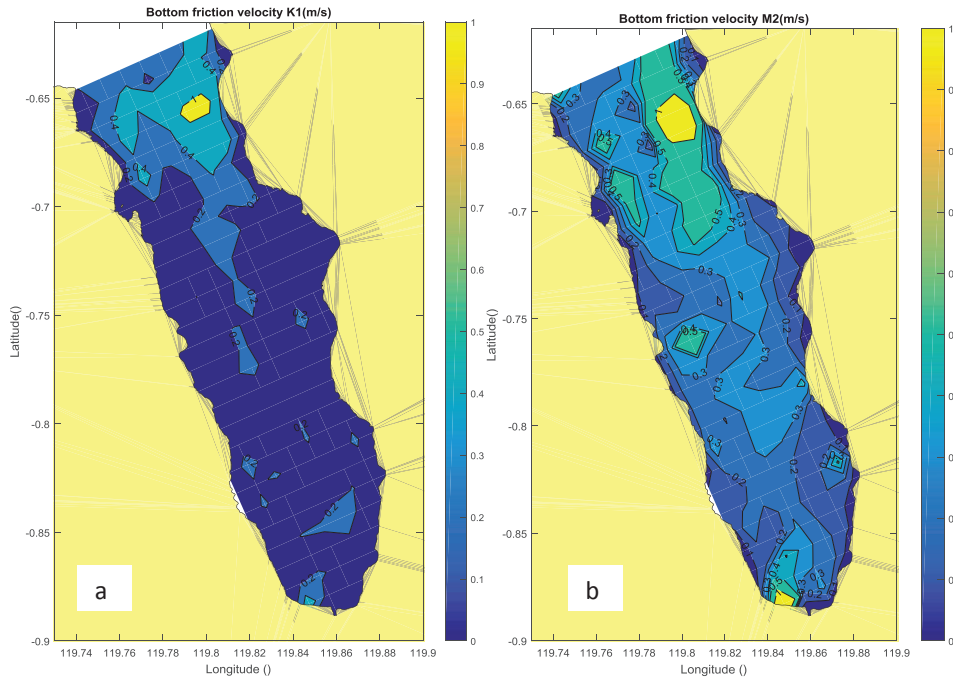

Fig. 8: Bottom friction velocity by (a) tidal constituent of K1, (b) tidal constituent of M2.
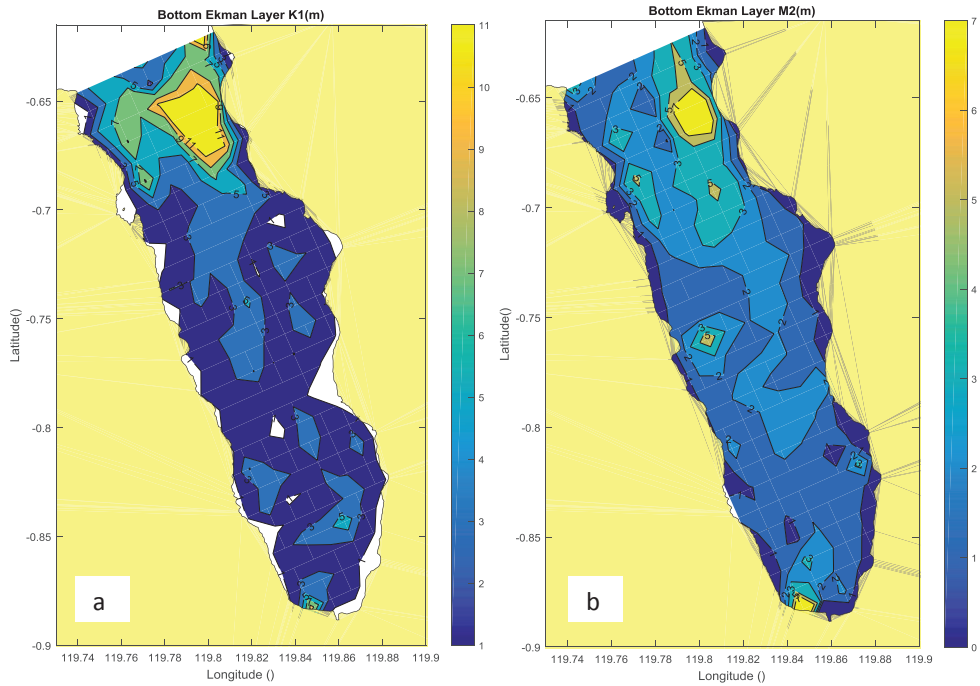
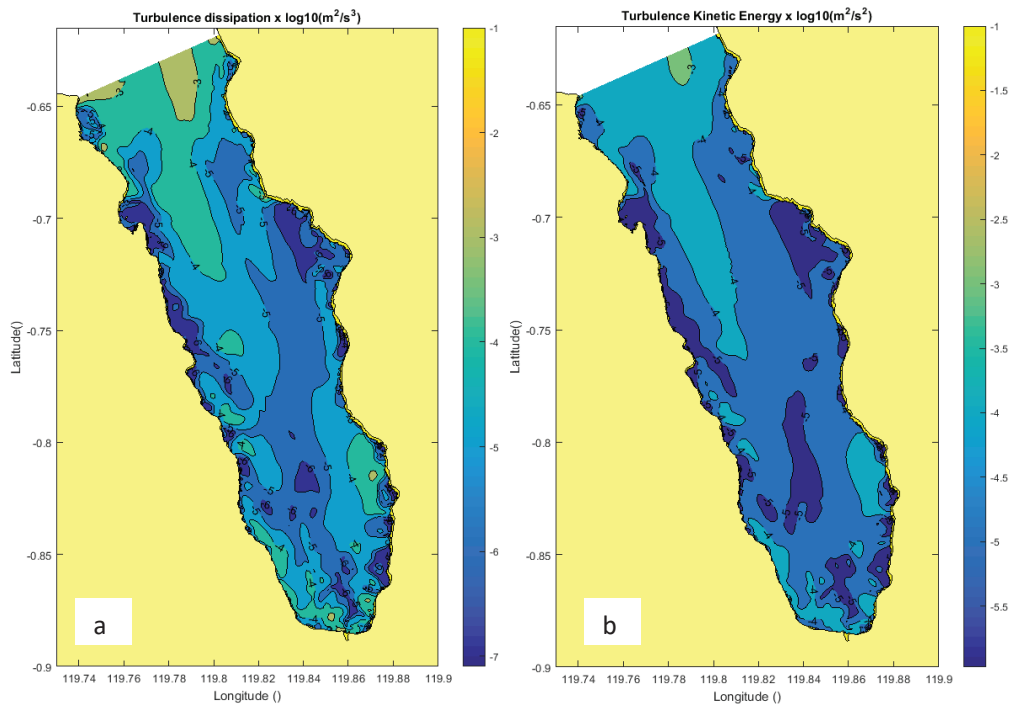Fig. 9: Bottom Ekman layer by (a) Tidal constituent of K1, and (b) Tidal constituent of M2.

Fig. 10 (a): Turbulent dissipation (ε) (b) turbulent kinetic energy Palu Bay.
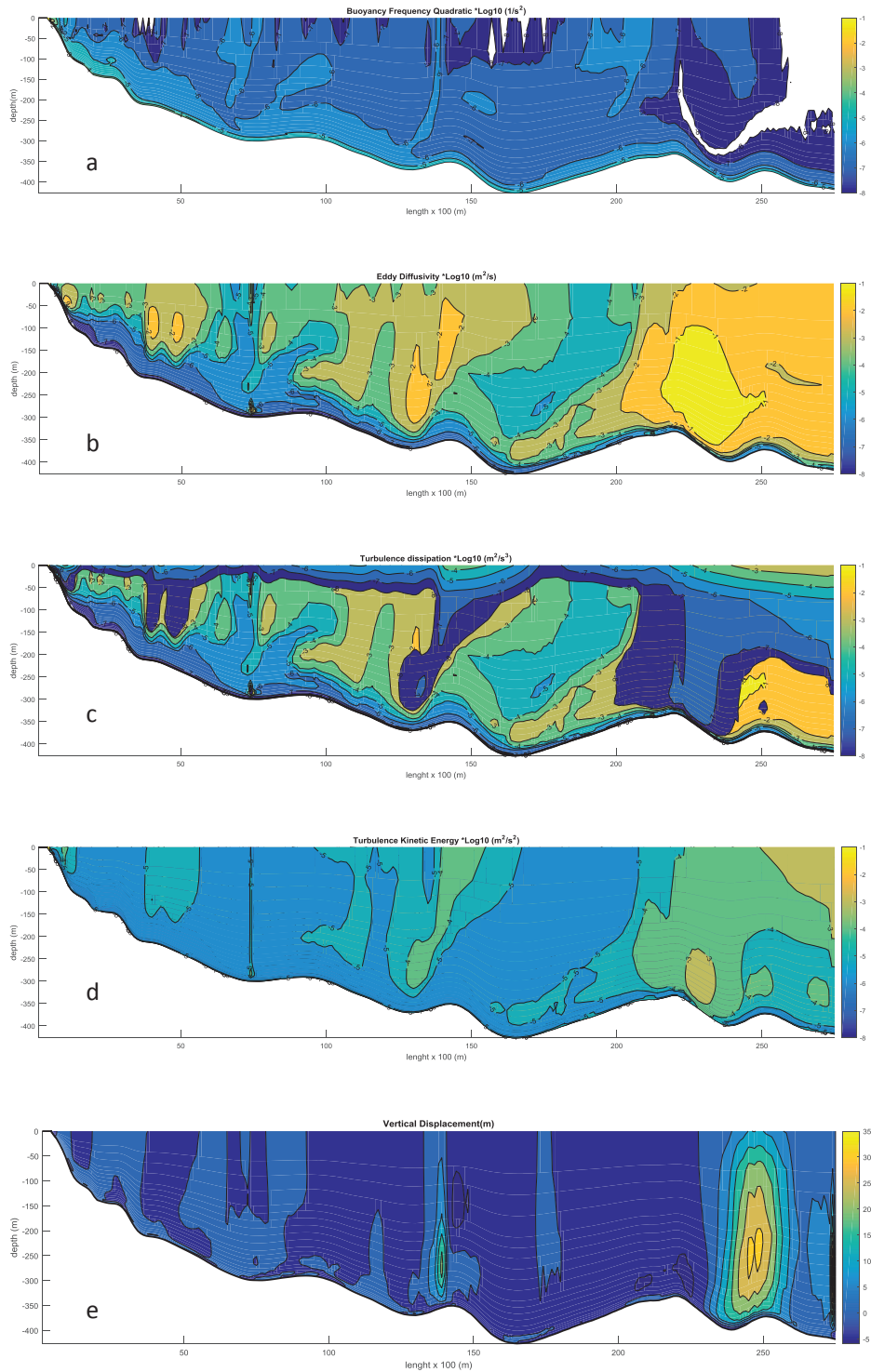
Fig. 11: Vertical slice of (a) buoyancy frequency, (b) eddy diffusivity, (c) turbulent dissipation, (d) turbulent kinetic energy, (e) vertical displacement in the waters of Palu Bay.

"η" is the elevation of the water level, "g" is acceleration of gravity, "h" is the depth of seawater, "T" is the period of tides, r_0 density of seawater. The results of the model show that M2 kinetic energy of turbulent (Fig. 7b) is greater than K1 (Fig. 7a) with the dominant energy vector to the north with large on the right side of Palu Bay.

Turbulent kinetic energy: The kinetic energy in Palu Bay is at O (10^{-5}-10^{-3}) with high kinetic energy found around the rough topography in the 10^{-3} order around the mouth of Palu Bay (Fig. 11d), the roughness effect tends to lower the average velocity distribution and increase turbulent kinetic energy within the boundary layer (Rachman et al. 2011).

CONCLUSION

The tidal elevation amplitude of the model K1 ranges from 19.27 to 19.31 cm, high tidal amplitude at the point near the mouth of the Palu River, and low tidal amplitude at the open boundary of the model that leads to the Makassar Strait. The amplitude range of M2 tidal constituents is 55.55 - 55.75 cm, high tidal amplitude at the mouth of Palu Bay and the end of Palu Bay and the slope area. The tidal current of the K1 constituent is strengthened at the open boundary of the model and weakened when it enters Palu Bay which then amplify near the mouth of the Palu River because of its extreme siltation. Tidal currents strengthen in the mouth area and the tip of Palu Bay by propagation of the tidal constituent M2 and the area in the slope along the coast of Palu Bay. The basic Ekman layer by the K1 constituent can reach 11 meters while the M2 constituent reaches 7 meters. In the slope area also found the buoyancy frequency with the order of 10^{-5} which is at a depth of 75-150 m. The kinetic energy in Palu Bay stands at O (10^{-5}-10^{-3}) with the highest kinetic energy found in the rough topography of the mouth of Palu Bay in the order of 10^{-3}.

REFERENCES

Baumert, H.Z., Simpson, J. and Sündermann, J. 2005. Marine Turbulence: Theories, Observations, and Models. Cambridge University Press.

Bayong T. 1999. Klimatologi Umum. Penerbit ITB Bandung.

Carbajal, N. and Backhaus, J. 1998. Simulation of tides, residual flow and energy budget in the Gulf of California. Oceanologica Acta., 21(3): 429-446.

Fortin, W.F., Holbrook, W.S. and Schmitt RW. 2016. Mapping turbulent diffusivity associated with oceanic internal lee waves offshore Costa Rica. Ocean Sci., 12: 601-612.

Gargett, A.E. and Holloway, G. 1984. Dissipation and diffusion by internal wave breaking. Journal of Marine Research, 42(1):15-27.

He, R. and Weisberg, R.H. 2002. Tides on the west Florida shelf. J. of Physical Oceanography, 32(12): 3455-3473.

Holt, J., Butenschon M., Wakelin S., Artioli Y. and Allen J. 2012. Oceanic controls on the primary production of the northwest European continental shelf: Model experiments under recent past conditions and a potential future scenario. Biogeosciences, 9: 97-117.

Hordoir, R., Höglund, A., Pemberton, P. and Schimanke, S. 2018. Sensitivity of the overturning circulation of the Baltic Sea to climate change, a numerical experiment. Climate Dynamics, 50(3-4): 1425-1437.

Jayne, S.R. and St Laurent, L.C. 2001. Parameterizing tidal dissipation over rough topography. Geophysical Research Letters, 28(5): 811-814.

Kartadikaria, A., Miyazawa, Y., Varlamov, S. and Nadaoka, K. 2011. Ocean circulation for the Indonesian seas driven by tides and atmospheric forcings: Comparison to observational data. Journal of Geophysical Research: Oceans, 116(C9).

Koropitan, A.F. and Ikeda, M. 2008. Three-dimensional modelling of tidal circulation and mixing over the Java Sea. Journal of Oceanography, 64(1): 61-80.

Ledwell, J., Montgomery, E., Polzin, K., Laurent, L.S., Schmitt, R. and Toole, J. 2000 Evidence for enhanced mixing over rough topography in the abyssal ocean. Nature, 403(6766): 179.

Lyard, F., Lefevre, F., Letellier, T. and Francis, O. 2006. Modelling the global ocean tides: Modern insights from FES2004. Ocean Dynamics, 56(5-6): 394-415.

Marín, V.H., Tironi, A., Paredes, M.A. and Contreras, M. 2013. Modelling suspended solids in a Northern Chilean Patagonia glacier-fed fjord: GLOF scenarios under climate change conditions. Ecological Modelling, 264: 7-16.

McGowan, J.A. and Hayward, T.L. 1978. Mixing and oceanic productivity. Deep Sea Research, 25(9): 771-793.

Merrifield, M.A. and Holloway, P.E. 2002. Model estimates of M2 internal tide energetics at the Hawaiian Ridge. Journal of Geophysical Research: Oceans, 107(C8): 5-1-5-12.

Nagai, T. and Hibiya, T. 2015. Internal tides and associated vertical mixing in the Indonesian Archipelago. Journal of Geophysical Research: Oceans, 120(5): 3373-3390.

Nash, J.D., Kunze, E., Toole, J.M. and Schmitt, R.W. 2004. Internal tide reflection and turbulent mixing on the continental slope. Journal of Physical Oceanography, 34(5): 1117-1134.

Neves, R. 2007. Numerical models as decision support tools in coastal areas. In: Di Dalam (ed.) Assessment of the Fate and Effects of Toxic Agents on Water Resources, Springer, pp. 171-195.

Nikurashin, M., Vallis, G.K. and Adcroft, A. 2013. Routes to energy dissipation for geostrophic flows in the Southern Ocean. Nature Geoscience, 6(1): 48.

Pawlowicz, R., Beardsley, B. and Lentz, S. 2002. Classical tidal harmonic analysis including error estimates in MATLAB using T_TIDE. Computers & Geosciences, 28(8): 929-937.

Pichon, A. and Correard, S. 2006. Internal tides modelling in the Bay of Biscay. Comparisons with observations. Scientia Marina, 70(S1): 65-88.

Pingree, R.D. and Mardell, G. 1981. Slope turbulence, internal waves and phytoplankton growth at the Celtic Sea shelf-break. Phil. Trans. R. Soc. Lond. A., 302(1472): 663-682.

Rachman, T., Suntoyo, S., Sambodho, K., Armono, H.D. and Yusroni, E. 2011. Numerical modelling of turbulent bottom boundary layer over rough bed under irregular waves. IPTEK The Journal for Technology and Science, 22(4): 177-189.

Robertson, R. and Ffield, A. 2005. M2 Baroclinic tides in the Indonesian seas. Oceanography-Washington Dc-Oceanography Society, 18(4): 62.

Rusdin, A., Abu, A., R. Kalawawo, P. 2014. Effect of debit on Palu River based sediment movements. National Civil Engineering Conference.

Sabhan, Koropitan A. F., Purba M., Pranowo W. S., Rusydi M. 2019 Numerical model of ocean currents, sediment transport, and geomorphology due to reclamation planning in Palu Bay. AES Bioflux 11(2): 87-96.

Schafstall, J., Dengler, M., Brandt, P. and Bange, H. 2010. Tidal induced mixing and diapycnal nutrient fluxes in the Mauritanian upwelling region. Journal of Geophysical Research: Oceans, 115(C10).

Sharples, J., Moore, C.M. and Abraham, E.R. 2001. Internal tide dissipation, mixing, and vertical nitrate flux at the shelf edge of NE New Zealand. Journal of Geophysical Research: Oceans, 106(C7): 14069-14081.

Toole, J.M., Schmitt, R.W. and Polzin, K.L. 1994. Estimates of diapycnal mixing in the abyssal ocean. Science, 264(5162): 1120-1123.

Versteeg, H.K. and Malalasekera, W. 2007. An Introduction to Computational Fluid Dynamics: The Finite Volume Method. Pearson Education, Pearson Education Limited

Wunsch, C. 1968. On the propagation of internal waves up a slope. Deep Sea Research and Oceanographic, 15: 251-258.

Xing, J. and Davies, A.M. 2009. Influence of bottom frictional effects in sill regions upon lee wave generation and implications for internal mixing. Ocean Dynamics, 59(6): 837-861.

Zhurbas, V., Väli, G., Golenko, M. and Paka, V. 2018. Variability of bottom friction velocity along the inflow water pathway in the Baltic Sea. Journal of Marine Systems, 184: 50-58.